

# Analysis of Tumor Microenvironment Changes after Neoadjuvant Chemotherapy with or without Bevacizumab in Advanced Ovarian Cancer (GEICO-89T/MINOVA Study)



Beatriz Tavira<sup>1,2,3</sup>, Teresa Iscar<sup>4</sup>, Luis Manso<sup>5</sup>, Ana Santaballa<sup>6</sup>, Marta Gil-Martin<sup>7</sup>, Yolanda García García<sup>8</sup>, Margarita Romeo<sup>9</sup>, Maria Iglesias<sup>10</sup>, Ana de Juan Ferré<sup>11</sup>, María Pilar Barretina-Ginesta<sup>12</sup>, Aranzazu Manzano<sup>13</sup>, Lydia Gaba<sup>14</sup>, María Jesús Rubio<sup>15</sup>, Carlos E. de Andrea<sup>4,16</sup>, and Antonio González-Martín<sup>1,17</sup>

## ABSTRACT

**Purpose:** The aim of our study was to elucidate the impact of bevacizumab added to neoadjuvant chemotherapy (NACT) on the tumor immune microenvironment and correlate the changes with the clinical outcome of the patients.

**Experimental Design:** IHC and multiplex immunofluorescence for lymphoid and myeloid lineage markers were performed in matched tumor samples from 23 patients with ovarian cancer enrolled in GEICO 1205/NOVA clinical study before NACT and at the time of interval cytoreductive surgery.

**Results:** Our results showed that the addition of bevacizumab to NACT plays a role mainly on lymphoid populations at the stromal compartment, detecting a significant decrease of CD4<sup>+</sup> T cells, an increase of CD8<sup>+</sup> T cells, and an upregulation in effector/regulatory cell ratio (CD8<sup>+</sup>/CD4<sup>+</sup>FOXP3<sup>+</sup>). None of the changes observed were detected in the intra-epithelial site in any arm

(NACT or NACT-bevacizumab). No differences were found in myeloid lineage (macrophage-like). The percentage of Treg populations and effector/regulatory cell ratio in the stroma were the only two variables significantly associated with progression-free survival (PFS).

**Conclusions:** The addition of bevacizumab to NACT did not have an impact on PFS in the GEICO 1205 study. However, at the cellular level, changes in CD4<sup>+</sup>, CD8<sup>+</sup> lymphocyte populations, and CD8<sup>+</sup>/CD4<sup>+</sup>FOXP3 ratio have been detected only at the stromal site. On the basis of our results, we hypothesize about the existence of mechanisms of resistance that could prevent the trafficking of T-effector cells into the epithelial component of the tumor as a potential explanation for the lack of efficacy of ICI in the first-line treatment of advanced epithelial ovarian cancer.

See related commentary by Soberanis Pina and Oza, p. 12

<sup>1</sup>Laboratory of Translational Oncology, Program in Solid Tumors, Cima-Universidad de Navarra, Cancer Center Clínica Universidad de Navarra (CCUN), Pamplona, Spain. <sup>2</sup>Navarra Institute for Health Research (IdiSNA), Pamplona, Spain. <sup>3</sup>Department of Pathology, Anatomy and Physiology, School of Medicine, University of Navarra, Pamplona, Spain. <sup>4</sup>Department of Pathology, Cancer Center Clínica Universidad de Navarra, Madrid, Spain. <sup>5</sup>Department of Medical Oncology, Hospital 12 de Octubre, Madrid, Spain. <sup>6</sup>Department of Medical Oncology, Hospital Universitario y Politécnico La Fe, Valencia, Spain. <sup>7</sup>Department of Medical Oncology, Institut Català d'Oncologia L'Hospitalet, Hospitalet de Llobregat, Spain. <sup>8</sup>Department of Medical Oncology, Parc Taulí Parc Taulí Hospital Universitari, Institut d'Investigació i Innovació Parc Taulí (I3PT), Universitat Autònoma de Barcelona, Sabadell, Spain. <sup>9</sup>Department of Medical Oncology, Institut Català d'Oncologia Badalona, Badalona, Spain. <sup>10</sup>Department of Medical Oncology, Hospital Son Llàtzer, Palma de Mallorca, Spain. <sup>11</sup>Department of Medical Oncology, Hospital Marqués de Valdecilla, Santander, Spain. <sup>12</sup>Department of Medical Oncology, Institut Català d'Oncologia Girona, Girona, Spain. <sup>13</sup>Department of Medical Oncology, Hospital Clínico San Carlos, Madrid, Spain. <sup>14</sup>Department of Medical Oncology, Hospital Clínic de Barcelona, Barcelona, Spain. <sup>15</sup>Department of Medical Oncology, Hospital Universitario Reina Sofía, Córdoba, Spain. <sup>16</sup>Centro de Investigación Biomédica en Red de Cáncer (CIBERONC), Madrid, Spain. <sup>17</sup>Department of Medical Oncology, Cancer Center Clínica Universidad de Navarra, Madrid, Spain.

**Corresponding Author:** Antonio González-Martín, Medical Oncology, Clínica Universidad de Navarra, Madrid 28027, Spain. E-mail: agonzalezma@unav.es

Clin Cancer Res 2024;30:176–86

doi: 10.1158/1078-0432.CCR-23-0771

This open access article is distributed under the Creative Commons Attribution-NonCommercial-NoDerivatives 4.0 International (CC BY-NC-ND 4.0) license.

©2023 The Authors; Published by the American Association for Cancer Research

## Introduction

Advanced epithelial ovarian cancer (EOC) is still the leading cause of death related to gynecologic cancer in non-middle- or low-income countries. Primary cytoreductive surgery (PCS) with the aim of complete cytoreduction followed by systemic therapy is considered the preferred option in the management of newly diagnosed advanced EOC. When PCS is not feasible due to the extension of disease properly assessed by an expert Gynecological Oncological team, neoadjuvant chemotherapy (NACT) followed by interval cytoreductive surgery (ICS) is considered a valid alternative (1–4). The efficacy of bevacizumab, a humanized anti-VEGF antibody, added to first-line paclitaxel-carboplatin-based chemotherapy after PCS was well established in the GOG-218 and ICON-7 clinical trials that showed an incremental benefit in progression-free survival (PFS; refs. 5, 6). In addition, two randomized phase II trials evaluated the addition of bevacizumab to NACT before ICS (7, 8). The GEICO 1205/NOVA study (NCT01847677), sponsored by Grupo Español de Investigación en Cáncer de Ovario (GEICO), failed to demonstrate an improvement in the rate of complete macroscopic response at ICS, optimal cytoreduction, or PFS with the addition of bevacizumab to NACT but confirmed that it was feasible.

VEGF blockade may promote T-cell infiltration into the tumor bed and reduce immunosuppression within the tumor microenvironment (TME), providing the rationale to combine immunotherapeutic and antiangiogenic strategies in tumors associated with increased VEGF production, such as EOC. Unfortunately, the addition of atezolizumab (a humanized anti-PD-L1 antibody) to standard first-line systemic

### Translational Relevance

Our study of immunohistochemistry and multiplex immunofluorescence, with spatial differentiation between stroma and tumor in paired matched samples of the GEICO1205/NOVA trial, has shown that the addition of bevacizumab to neoadjuvant chemotherapy in advanced ovarian cancer significantly decreased CD4<sup>+</sup> T cells, increased CD8<sup>+</sup> T cells, and upregulated the effector/regulatory cell ratio (CD8<sup>+</sup>/CD4<sup>+</sup>FOXP3<sup>+</sup>). However, these changes have been observed only in the stromal compartment and not at the intra-epithelial level. Our findings suggest the existence of mechanisms of resistance that could prevent the trafficking of T-effector cells into the epithelial component of the tumor as a potential explanation for the lack of efficacy of adding immune check-point inhibitors to chemotherapy with bevacizumab in the first-line treatment of advanced epithelial ovarian cancer.

therapy with paclitaxel, carboplatin, and bevacizumab after PCS or NACT did not improve the PFS, and translational research may help to understand why this combination did not work (9).

Recent studies have described an increment in tumor-infiltrating leukocyte (TIL) and natural killer (NK) infiltration in addition to PD-L1 expression after NACT in the TME (10, 11). In this context, the presence of specific T-cell subpopulations has been consistently associated with better or worst prognosis in patients with ovarian cancer. Particularly, the presence CD8<sup>+</sup> cytotoxic cells have been linked to better clinical outcome meanwhile regulatory T cells (CD4<sup>+</sup>FOXP3<sup>+</sup> phenotype) are often associated with negative prognostic (12–14). Similarly, the balance between M1/M2 tumor-associated macrophages (TAM, CD163<sup>+</sup>CD204<sup>+</sup> for M2) have shown to predict the prognosis of the patients being related to tumor progression and chemoresistance in EOC (15).

In this context, GEICO 1205 study provided the opportunity of analyzing the changes in the TME induced by chemotherapy with or without bevacizumab in the paired matched samples obtained at baseline and at ICS and correlate the changes with the clinical outcome of the patients.

## Materials and Methods

### Trial design and treatment

The GEICO 1205/NOVA study was a double arm, open-label, and randomized phase II multicentric clinical trial to determine the efficacy and toxicity of preoperative chemotherapy without (control arm) or with bevacizumab (experimental arm) in patients with AOC (NCT01847677). The clinical trial was conducted in 11 centers in Spain from May 2013 to May 2019 and was sponsored by GEICO. All patients included provided informed written consent before participation. Eligible patients were ages  $\geq 18$  years with newly diagnosed unresectable International Federation of Gynecology and Obstetrics (FIGO) stage III or IV high-grade serous or endometrioid epithelial ovarian, primary peritoneal, or fallopian tube carcinoma, Eastern Cooperative Oncology Group (ECOG) performance status of 0 to 2 and were considered candidates for neoadjuvant chemotherapy followed by IDS. This study has been conducted in accordance with the Declaration of Helsinki Ethical Guidelines.

Patients were randomized 1:1 to receive four neoadjuvant cycles of chemotherapy (carboplatin AUC 6 and paclitaxel 175 mg/m<sup>2</sup>, repeated every 3 weeks) either alone or with at least three cycles of bevacizumab

15 mg/kg every 3 weeks. After ICS, all patients (investigational and control arm) received three cycles of the same chemotherapy and bevacizumab, followed by single-agent bevacizumab up to 15 months of treatment. Bevacizumab was omitted from any cycles given within 28 days before or after surgery (Fig. 1). The study was conducted in accordance with the Declaration of Helsinki Ethical Guidelines.

The translational study we present was approved by the Spanish Agency for Medicines and Medical Products (AEMPS) on July 09, 2020, and the Ethics Committee for Investigation with medicinal products (CEIm at Parc Tauli Hospital) on September 25, 2020. All the patients provided written informed consent.

### Formalin-fixed paraffin-embedded (FFPE) tissue specimens

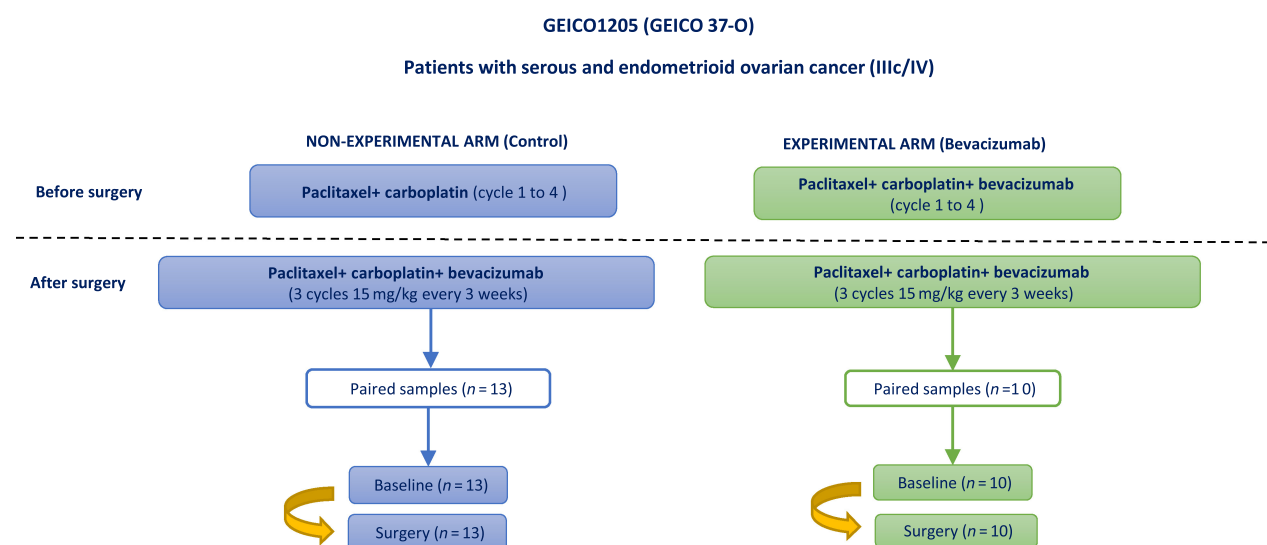
FFPE tumor samples from primary (ovary) or metastatic sites (e.g., peritoneum, omentum) were collected from patients before NACT and at the time of ICS (Supplementary Table S1). From each patient, five sequential 4  $\mu$ m sections from the specimen were available to be used for conventional IHC, monoplex and multiplex immunofluorescence (IF) validation. Hematoxylin-eosin IHC staining was performed in the entire cohort to determine the region of interest (ROI) of each slide for multispectral imagen.

### IHC and multiplex IF

Human tonsil FFPE tissue with and without primary antibodies was used as positive and negative control for each IHC staining. The correct titrations of each antibody present in “Opal 7 Solid Tumor Immunology Kit” (OP7TL4001KT; Akoya Bioscience) were chosen based on the concentrations used in the positive and negative staining in the control, obtaining a uniform and specific cell staining for each marker. Monoplex IF assay was performed using two ovarian cancer samples, to optimize the antibodies and generate spectral libraries required for the multiplex image analysis in the same type of tissue. For the sampling processing, an automated staining system, BOND-MAX (Leica Microsystem) was used to perform multiplex IF according to the manufacturer's instructions. SciScore report displayed a value of 5 and suggested the follow research resource identifiers (RRID) for specific markers included in addition to the ones used in our study. The kit includes antibodies against: CD4 (FE1600–80  $\mu$ L, dilution 1:100, Opal 520, Nanostring Catalog No. 121300104, RRID: AB\_2893077), CD8 (FP1601–30  $\mu$ L, dilution 1:300, Opal 570, Bethyl Catalog No. A810–004, RRID:AB\_2891975), CD68 [FP1606–10  $\mu$ L, dilution 1:250, Opal 650, LSBio (LifeSpan) Catalog No. LS-C5468–1000, RRID:AB\_10638461], FoxP3 (FP1605–40  $\mu$ L, dilution 1:1,000, Opal 620), pancytokeratin AE1/AE3 (epithelial cell positive, dilution 1:500, Opal 690), Spectral DAPI (FP1490). Additional studies in tumoral macrophages population (TAM) to distinguish between M1/M2 like-class was performed using “Opal 7 color manual IHC kit 50 slides” in combination with antibodies for CD68<sup>+</sup> (Abcam, dilution 1:1,000, nonspecific marker for macrophages, Leica Biosystems Catalog No. RTU-CD68, RRID:AB\_563624) and CD163<sup>+</sup> (Abcam, dilution 1:100, M2-like macrophage), pancytokeratin AE1/AE3 (epithelial cell positive, dilution 1:500, Opal 690), Spectral DAPI (FP1490). According to the literature, CD68<sup>+</sup> was chosen as a non-specific macrophage marker and CD163<sup>+</sup> as a putative marker for M2-polarized protumoral macrophages (16).

### Image collection and analysis

Sample scanning (20 $\times$ ), ROIs selection, and spectral unmixing were conducted with Vectra Polaris Quantitative Pathology Imaging System (v1.0.13) using Phenochart (v1.0.12) and InForm 2.5.1 software (Akoya Biosciences), respectively. Histologic assessment of

**Figure 1.**

Design of the clinical trial GEICO1205. Patients with ovarian cancer in stage IIIc/IV were initially treated with chemotherapy based on paclitaxel and carboplatin in both arms. Experimental arm was treated with bevacizumab in addition to the previous chemotherapy scheme. After surgery, both groups received bevacizumab every 3 weeks. In this study, matched samples pre- and postsurgery were analyzed to study the potential changes in the TME related to the differential treatment. This figure has been created on the basis of the information published in the article by García García and colleagues (8).

each sample was performed by the Anatomy & Pathology Department and several ROIs were selected (up to 20 maximum) to create a single image, capturing intra-epithelial and stromal areas in a whole picture. Further information regarding image selection and criteria is described in detail in Supplementary Materials and Methods. Bioimage analysis was carried out in the open-source software QuPath v 0.3.2 (17) and whole images per patient were built with the script “stitching.groovy” in the running console. All the immune cell populations were characterized and quantified by compartment (intra-epithelial and stromal) by segmenting the image tissue into tumor (defined by the presence of cytokeratin) and into stroma (absence of cytokeratin). Subsequently, cell segmentation was carried out using the pixel classification tool, cell detection, and object classification. The phenotyping of each cell subtype was performed on the basis of the selection of at least 100 spots corresponding to each of the markers analyzed in our panels ( $CD4^+$ ,  $CD8^+$ ,  $CD4^+FOXP3^+$  etc.) with the aim of carrying out the training of the software. Data were given as the percentage of the number of cells from a specific subpopulation/total number of cells present in each compartment.

### Statistical analysis

Continuous variables were represented as the median and interquartile range (IQR) according to normality data distribution (Kolmogorov–Smirnov test). In normal distributed variables (age, CA-125 values), *T* test was used to detect significant differences between the two groups while the Mann–Whitney test was used for non-normal distributed variables. Wilcoxon test was used to analyze differences between paired observations pre- and postsurgery. To compare three groups or more, ANOVA and Kruskal–Wallis test were performed for normally and non-normally distributed data, respectively. Progression-free survival (PFS) was calculated from the date of the first chemotherapy cycle to the date of the end of the study using the Kaplan–Meier method and analysis was performed with a Mantel–Cox model (log-rank) as described

previously (8). Pearson correlations were performed to determine whether the patient’s clinical outcome was associated with continuous variables. GraphPad Prism 7 (GraphPad Software, RRID: SCR\_002798) was used to perform the computations and graphics for all analyses.

### Data availability

The data generated in this study are not publicly available to guarantee the confidentiality and privacy of clinical data from patients but are available upon reasonable request from the corresponding author.

## Results

A total number of 23 matched samples (13 patients in the control arm/10 patients in the bevacizumab arm, total  $n = 46$ ) of 71 patients included, from primary (ovary) or metastatic sites (e.g., peritoneum, omentum) were finally available for the study. The samples were paired by the patient but not by tumor site, mainly due to the absence of tumor at the same location after NACT or inadequate quality of the sample. The quality of the sample or the absence of one paired sample were the most frequent reasons for the lack of available samples (Supplementary Fig. S1).

### Patient characteristics and clinical outcome

Patients included in GEICO-1205 were Caucasian. Clinical characteristics according to the treatment arm are detailed in Supplementary Table S1. No significant differences were found between the control and the bevacizumab group in variables described previously (8). The median age was 64 years, and all patients presented with FIGO stage IIIc or IV. The most frequent histological subtype was HGSOC in 75% of the patients and 95.8% presented grade 3 (poorly differentiated) tumor. The median PFS was 22.57 months in the control arm and 21.36 months in the bevacizumab arm.

**Changes in T cells and TAMs subpopulations in intra-epithelial and stromal compartments after neo-adjuvant chemotherapy with bevacizumab**

Total helper CD4<sup>+</sup> T cells (CD4<sup>+</sup>Th) were evaluated in the intra-epithelial and stromal compartments in each treatment group at primary diagnosis and ICS. No significant differences in the intra-epithelial site were detected between the control and bevacizu-

mab groups before and after NACT. In contrast, a reduction in CD4<sup>+</sup>Th cells in the stromal site was observed after NACT, being statistically significant in the bevacizumab group but not in the control arm (Mann-Whitney test,  $P = 0.028$ , Fig. 2A). Matched paired samples confirmed these results, observing a remarkable decrease in CD4<sup>+</sup>Th cells in most of the patients analyzed (Wilcoxon test,  $P = 0.0098$ , Fig. 2B).

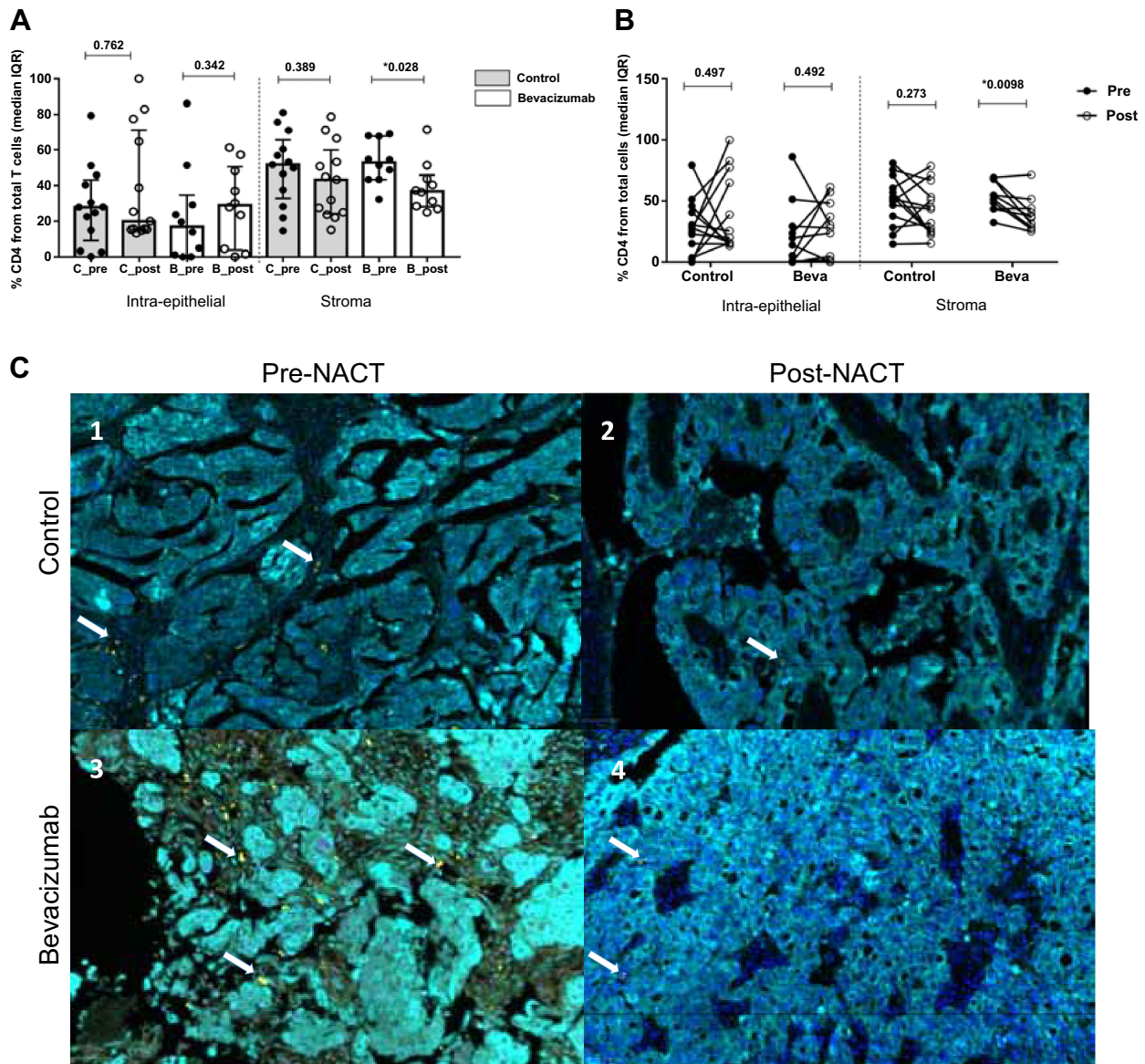


**Figure 2.** Analysis of CD4<sup>+</sup> T-cell immune infiltrates in patients with epithelial ovarian cancer. **A**, Cellular percentages of CD4<sup>+</sup> T cells present in the intraepithelial and stromal compartment. Values are given as median and IQR. Mann-Whitney test was used to compare differences in the general population according to the treatment and the time of surgery. After chemotherapy, helper CD4<sup>+</sup> T-cell populations experienced a decrement being statistically significant in the stromal compartment for the bevacizumab arm ( $P = 0.028$ ) (Imagen c3 vs. c4). **B**, Differences between pre-NACT (black dots) and post-NACT (white dots) samples were analyzed. Changes in paired match samples were calculated with the Wilcoxon test. The results previously observed in CD4<sup>+</sup> Th populations were confirmed in the individual analysis, showing a decrement in the CD4<sup>+</sup> subpopulations after chemotherapy ( $P = 0.0098$ ). **C**, Representative images of multispectral for CD4<sup>+</sup> recruitment at intraepithelial (cytokeratin, Opal 690, blue) and stromal compartment (nuclei, DAPI) before and after NACT with bevacizumab. In each image, white arrows indicate CD4<sup>+</sup> positive cells (Opal 520, yellow). The images in our study correspond to four representative patients from each of the study groups (pre-post NACT, control, and bevacizumab group), for the CD4<sup>+</sup>, CD8<sup>+</sup>, CD4<sup>+</sup>FOXP3<sup>+</sup> populations present in each of these patients (same patient for different immune cell populations).

NACT induced no significant reduction of regulatory T cells (Treg) (phenotype  $CD4^+FOXP3^+$  double staining) at the intra-epithelial and the stroma compartment in both groups (Fig. 3A and B). Conversely, the cytotoxic  $CD8^+$  T-cell population increased in the post-NACT samples only in the stroma, reaching statistical significance in the bevacizumab arm but not in the control group (Fig. 4A,  $P = 0.028$ ). Individual analysis of paired matches samples confirmed these results, where post-NACT values of  $CD8^+$  cyto-

toxic T cells infiltration were significantly increased compared with pre-NACT samples (Fig. 4B).

Because of the relevance of the balance between the T effectors and T regulators cells in the tumor immune scenario, the ratio of  $CD8^+/CD4^+FOXP3^+$  cells was calculated. In our study, the proportion of  $CD8^+$  effector cells was higher at both intraepithelial and stromal compartments after NACT, reaching statistical significance in the stroma of patients within the bevacizumab group (Fig. 5A and B).

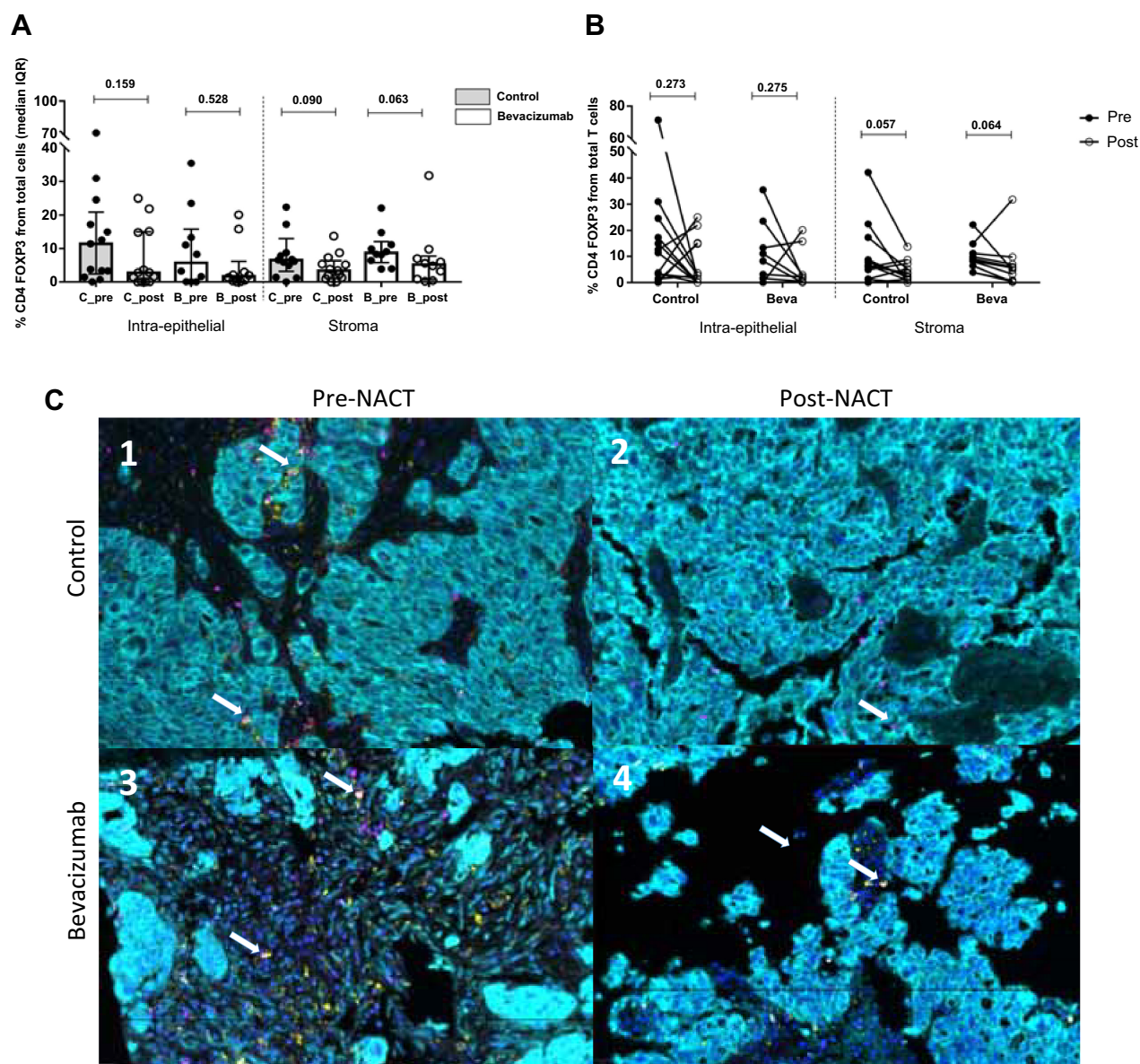


**Figure 3.**

Analysis of  $CD4^+FOXP3^+$  cells (Treg) in ovarian cancer samples. **A**,  $CD4^+FOXP3^+$  (Tregs, double staining) experienced a decrease in both compartments and treatment arms without being significant after NACT. Values are given as median and IQR. **B**, Differences in paired samples were calculated with the Wilcoxon test, observing the same tendency without being significant: reduction of Treg subpopulations after chemotherapy. **C**, Representative images of multispectral for  $CD4^+FOXP3^+$  recruitment at intraepithelial (cytokeratin, Opal 690, blue) and stromal compartment (nuclei, DAPI). In each image, white arrows indicate  $CD4^+$  positive cells (Opal 520, yellow) and  $FOXP3^+$  (Opal 620, pink). The images in our study correspond to four representative patients from each of the study groups (pre-post NACT, control, and bevacizumab group), for the  $CD4^+$ ,  $CD8^+$ ,  $CD4^+FOXP3^+$  populations present in each of these patients (same patient for different immune cell populations).

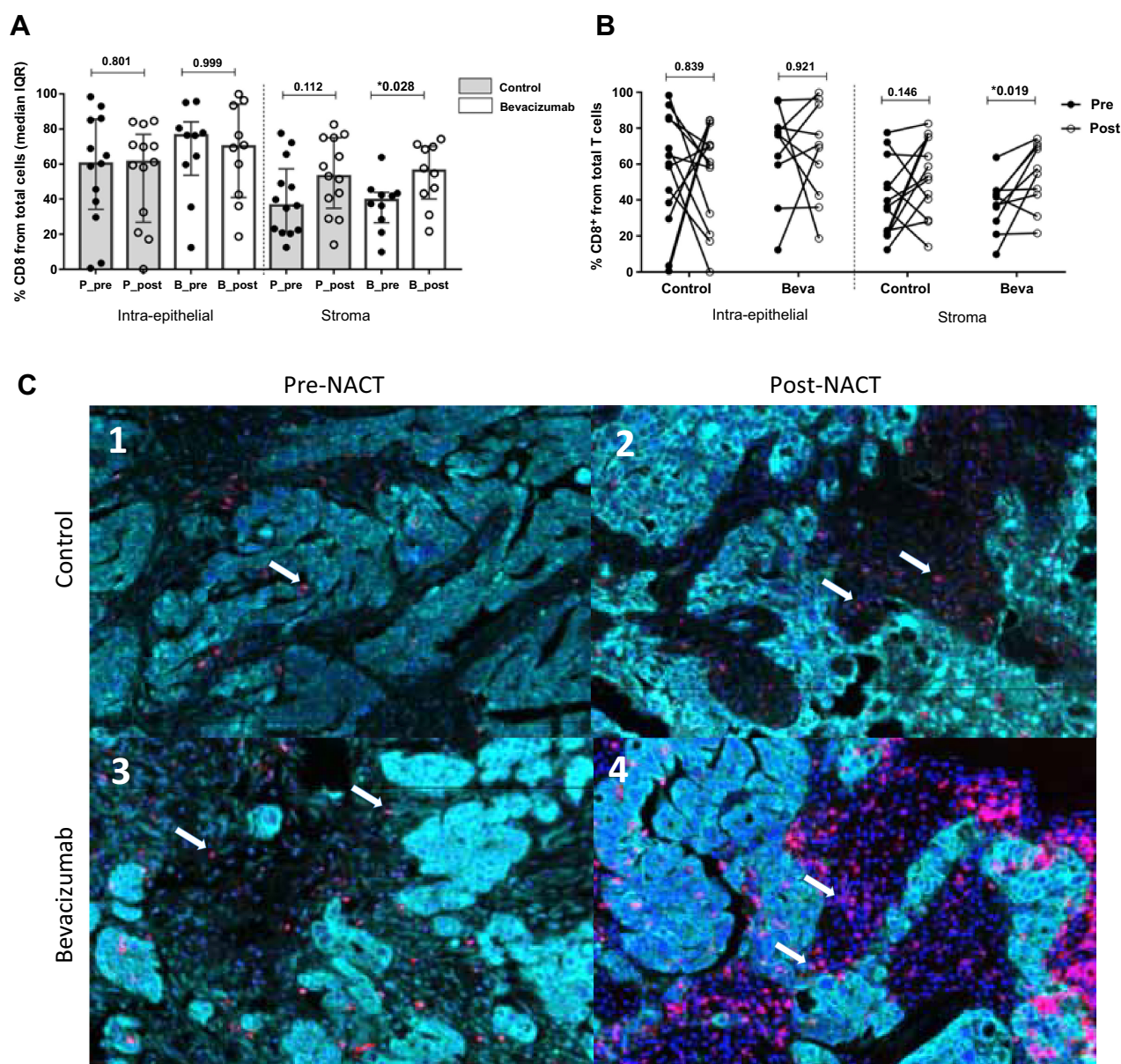


**Figure 4.**

Comparison of CD8<sup>+</sup> T-cell immune infiltration at stromal compartment. **A**, Cellular percentages in CD8<sup>+</sup> T present in the different compartments at ovarian cancer sample. Values are given as median and IQR. A significant increase of CD8<sup>+</sup> populations is observed in the stromal compartment in the bevacizumab group ( $P = 0.028$ , Mann-Whitney test). **B**, Individual variation from presurgery samples to postsurgery was calculated using the Wilcoxon test, displaying a significant increase over time in the NACT group with bevacizumab ( $P = 0.019$ ). **C**, Representative images from multispectral analysis of CD8<sup>+</sup> recruitment at tumor and stromal compartment before and after NACT with bevacizumab. In each image, white arrows indicate CD8<sup>+</sup> positive cells (Opal 570, red). In the control group, a slight increase is produced after NACT, being very remarkable the infiltration in the bevacizumab group after NACT (c3 vs. C4). The images in our study correspond to four representative patients from each of the study groups (pre-post NACT, control, and bevacizumab group), for the CD4<sup>+</sup>, CD8<sup>+</sup>, CD4<sup>+</sup>FOXP3<sup>+</sup> populations present in each of these patients (same patient for different immune cell populations).

TAMs cell subpopulations were defined as CD68<sup>+</sup>CD163<sup>-</sup> for M1-like macrophages and C68<sup>+</sup>CD163<sup>+</sup> for M2-like macrophages. No differences between both arms at any compartments, either for M1-like and M2-like markers were observed (Fig. 6A–C). Individual analysis pre- and post-NACT confirmed this observation in the intra-epithelial and the stromal sites in both treatment groups (Fig. 6B–D). Representative images of multispectral for helper T cells (CD4<sup>+</sup>), Treg (CD4<sup>+</sup>FOXP3<sup>+</sup>), cytotoxic T cells (CD8<sup>+</sup>) and TAMs (CD68, CD163)

recruitment at intra-epithelial and stromal compartment before and after NACT with bevacizumab are shown in Figs. 2C, 3C, 4C, and 6E, respectively.

#### Impact of T cells and TAMs subpopulations on PFS

The impact of immune cell infiltration present on intra-epithelial and stromal compartments on PFS was evaluated at the different time points (pre- and post-NACT) to elucidate their possible role as

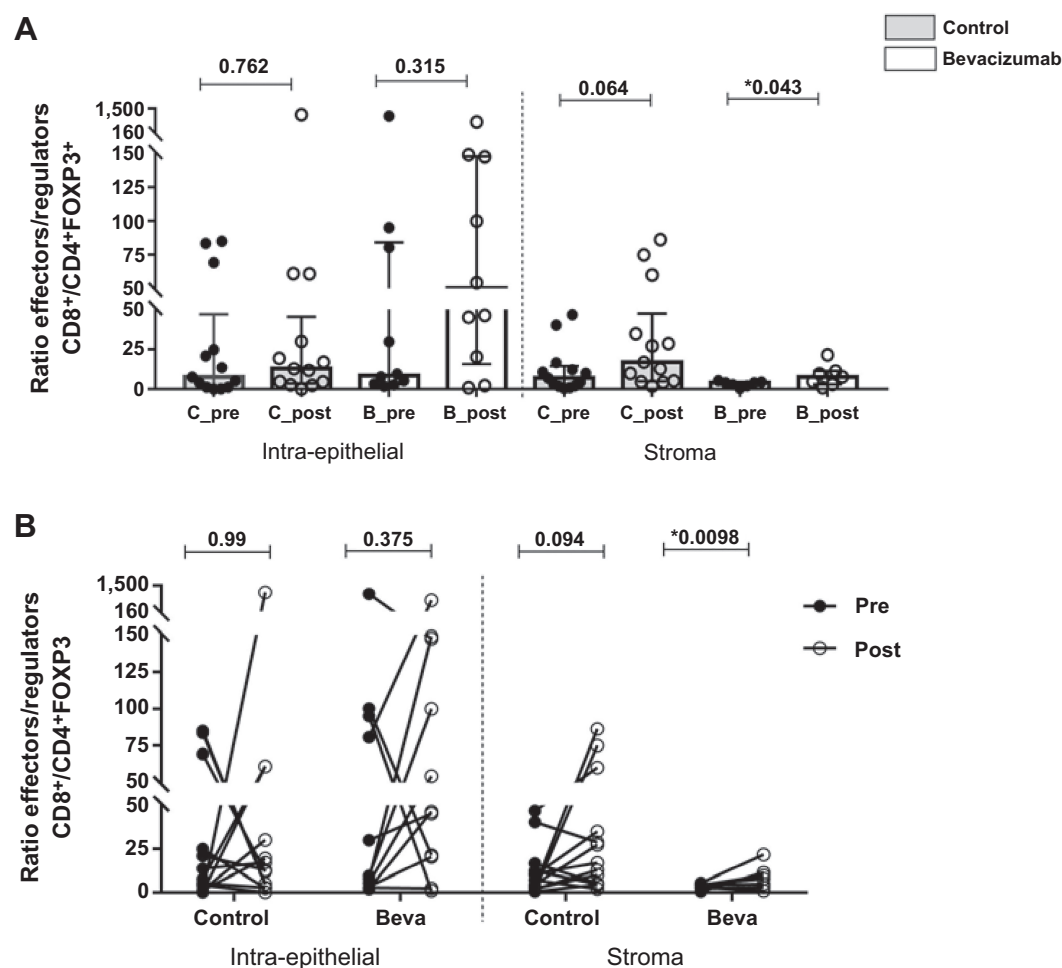


**Figure 5.**

Balance between effectors (CD8<sup>+</sup>) and regulatory cells (CD4<sup>+</sup>FOXP3<sup>+</sup>). **A**, Balance between cell effectors (cytotoxic CD8<sup>+</sup> cells) and regulators (CD4<sup>+</sup>FOXP3<sup>+</sup>, double staining) was calculated using cell ratio. The stromal compartment showed a greater percentage of effector cells in the bevacizumab arm when before and after NACT ratios were compared ( $P = 0.043$ , Mann-Whitney test). **B**, Individual analysis in the intra-epithelial site did not show any difference regarding the ratio between effector and regulator cells, displaying a strong association in the stromal site between pre- and postsurgery values in the bevacizumab group ( $P = 0.0098$ ). The images in our study correspond to four representative patients from each of the study groups [present in each of these patients (same patient for different immune cell populations: post NACT, control, and bevacizumab group), for the CD4<sup>+</sup>, CD8<sup>+</sup>, CD4<sup>+</sup>FOXP3<sup>+</sup> populations].

potential markers of the patient's clinical outcome related to each experimental arm. In pre-NACT samples, none of the T cell subsets detected in any compartment correlated with PFS (data not shown). On the contrary, an increment in the Treg population (CD4<sup>+</sup>FOXP3<sup>+</sup>) in the stroma after NACT correlated negatively with PFS (Supplementary Fig. S2A,  $P = 0.036$ ,  $r = -0.437$ ) for the overall population. However, this significance was driven by individuals included in the control group but not by the patients in the bevacizumab arm (Supplementary Fig. S2B,  $P = 0.04$ ,  $r = -0.577$  vs.  $P = 0.51$ ,  $r = -0.236$  respectively). Consistently, survival analysis in the overall population using Kaplan-Meier curves revealed that patients with a lower percentage of Treg at the stromal site after NACT (cut-off <4 median value) have longer PFS compared with those with higher infiltration of Tregs (Supplementary Fig. S2C,  $P = 0.015$ ).

None of the other stromal T-cell subsets (CD4<sup>+</sup> and CD8<sup>+</sup>) were linked to PFS after NACT. Because the balance between effector and suppressor immune cells could give relevant information about patient prognosis, we evaluated the correlation between the ratio of CD8<sup>+</sup>/

CD4<sup>+</sup>FOXP3<sup>+</sup> cells present in the intra-epithelial and stromal sites in post-NACT samples. This analysis showed that a higher ratio was associated with a better PFS in the overall population (Supplementary Fig. S3A). The Kaplan-Meier curves confirmed that patients with higher CD8<sup>+</sup>/CD4<sup>+</sup>FOXP3<sup>+</sup> ratios (median cut-off > 13) had better PFS (Supplementary Fig. S3b,  $P = 0.049$ ). Regarding the impact of TAMs on PFS, none of the markers for M1-M2 like showed any relationship with an extended PFS in any of the study arms before or after NACT.

## Discussion

The aim of this study was to characterize the immune subpopulations present in the TME after NACT with or without bevacizumab in patients diagnosed with advanced EOC. In our study, NACT including bevacizumab was associated with a significant decrease of CD4<sup>+</sup> T cells, an increase of CD8<sup>+</sup> T cells, and an upregulation effector/regulatory cells ratio (CD8<sup>+</sup>/CD4<sup>+</sup>FOXP3<sup>+</sup>) at the stromal

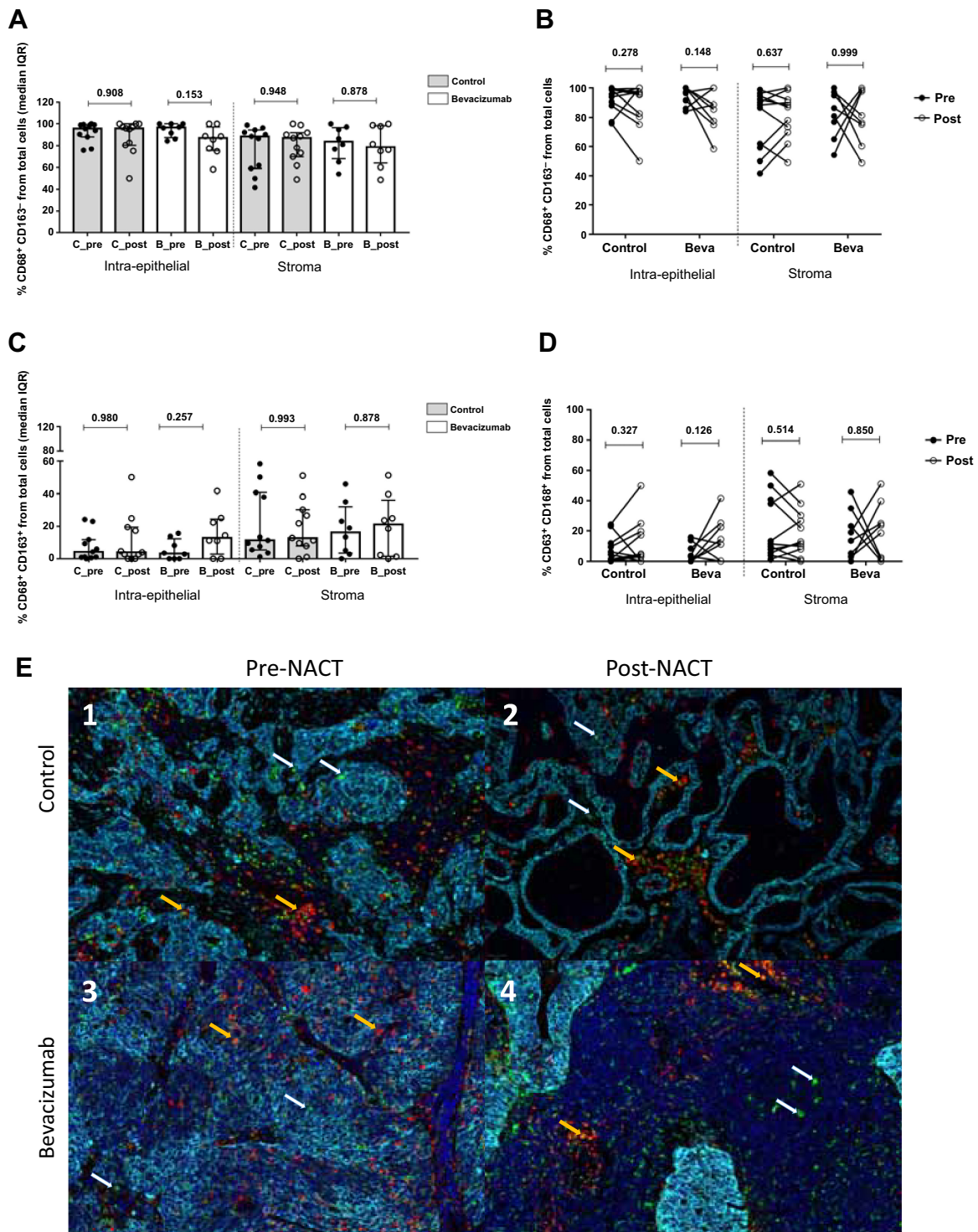


**Figure 6.** Analysis of TAM markers CD68<sup>+</sup> and CD163<sup>+</sup> present in patients with ovarian cancer in the intraepithelial and the stromal compartment. **A**, M1 markers (CD68<sup>+</sup>CD163<sup>-</sup>) did not present significant differences between pre- and postsurgery samples in any of the two groups (control and bevacizumab). **B**, Individual variation from pre-NACT samples to post-NACT was calculated using the Wilcoxon test and confirmed the tendency observed in the total population analysis. **C**, M2 markers (CD68<sup>+</sup>CD163<sup>+</sup>) showed less presence in the intraepithelial compartment than in the stroma, with no differences by experimental arm or time at surgery. **D**, Individual analysis confirmed the results previously obtained in the global population analysis. **E**, Multispectral images of CD68<sup>+</sup> and CD163<sup>+</sup> markers in representative samples from placebo (c1-c2) and bevacizumab (c3-c4) experimental groups. In each image, white arrows indicate CD68<sup>+</sup> positive cells, whereas orange arrows point to double staining CD68<sup>+</sup>CD163<sup>+</sup> as an M2-like phenotype.

compartment. These changes were not observed in the intra-epithelial site neither in the control arm nor the experimental arm with bevacizumab. No differences were found in the myeloid lineage (macrophages-like) defined by CD68<sup>+</sup> and CD163<sup>+</sup> markers.

TME is the scenario where tumor cells interact with various types of cells including immune cells, stromal cells, blood vessels, and extracellular matrix among others, maintaining an intense crosstalk promoting tumor growth and metastasis (18). The study of TME and its association with tumor response or resistance to current active drugs may help to develop new strategies for overcoming drug resistance and improving the patient's outcome. In this regard, the analysis of TME before and after NACT may provide substantial information. Several studies have analyzed the effect of NACT on TME in ovarian cancer showing an increment in B-cell and natural killer densities, a decrement of T regulatory density (CD4<sup>+</sup>FOXP3<sup>+</sup>), and the oligoclonal expansion of T cells (10, 19–21). In addition, NACT influences the expression of co-regulatory molecules in the TME as TIM3, IDO, PD-L1, and LAG3, all of them involved in the modulation of immunotolerance in ovarian cancer (22).

Anti-VEGF targeted therapy can play a major role in reversing the negative effects that VEGF secretion have in the TME either on angiogenesis, immunosuppression, or cell trafficking (23). However, there is no consistent information regarding the effect that bevacizumab displays on T cells in ovarian cancer. To our knowledge, only one previous study has tried to elucidate this question through the analysis of CD4<sup>+</sup>, CD8<sup>+</sup>, and CD4<sup>+</sup>FOXP3<sup>+</sup> (Treg) cells in PBMCs from patients with ovarian cancer that received NACT with bevacizumab showing an increase of CD8<sup>+</sup> population and reduction in circulating Treg over the time (24). These preliminary data need to be evaluated in the intraepithelial and stromal components of the tumor.

Our study performed in tumor-matched samples from patients with ovarian cancer before and after NACT with or without bevacizumab revealed a significant reduction of CD4<sup>+</sup> population in the stromal compartment only in the bevacizumab group, but this tendency was not detected in the intratumoral area. For several years, the presence of cytotoxic CD8<sup>+</sup> lymphocytes has been associated with better prognosis in patients with ovarian cancer meanwhile Treg correlated with the worst clinical outcome due to their suppressing role in the TME (25, 26). In our study, Treg levels undergo towards a general decrease either in the tumor and stroma compartment regardless of treatment arms (matched samples, control  $P = 0.057$ , bevacizumab  $P = 0.054$ ). This result goes in line with the ones observed in previous studies in ovarian cancer where the effect of NACT (without bevacizumab) on tumor-infiltrating lymphocyte populations demonstrated a significant reduction of CD4<sup>+</sup>FOXP3<sup>+</sup> cell population in the stromal compartment after NACT (21). We observed a longer PFS in patients with lower CD4<sup>+</sup>FOXP3<sup>+</sup> infiltration (below the median, <4) post-NACT in the stroma ( $P = 0.015$ ). This result is in line with prior studies performed with NACT in ovarian cancer (16, 20, 27).

However, in the analysis according to the treatment arm, this effect seems to be diluted by bevacizumab, and based on our results and the previous evidence, bevacizumab does not seem to potentiate the effect that NACT displays itself on Treg cells.

The analysis of effector cells (CD8<sup>+</sup> populations) after NACT with bevacizumab showed opposite results, detecting a higher infiltration of the CD8<sup>+</sup> population at the stroma compartment in the bevacizumab arm. The patients that did not receive anti-VEGF (control group) also experienced a higher expression of this cell type but without being statistically significant. These data agree with the results published in 2019 by Leary and colleagues, where they analyze the effect of NACT on TME. As in our study, the percentage of CD8<sup>+</sup> T cells increased at

the stromal level post-NACT, however, they also reported the same tendency at the intratumoral site (16). Despite this fact, they did not find any clinical correlation between the infiltration of CD8<sup>+</sup> in the tumor and PFS or overall survival (OS), which might indicate that not only tumoral infiltration but also cell functionality are determinant factors to take into consideration to achieve a successful antitumor effect.

Another important aspect to be considered is the balance between effectors/suppressor cells in the TME since the antitumor immunity depends on the proportion of each cell type. In our study, CD8<sup>+</sup>/CD4<sup>+</sup>FOXP3<sup>+</sup> ratios in matched samples increased after NACT regardless of treatment arm or location (tumor or stroma) but was only significant in the stromal site for the bevacizumab arm, and a higher CD8<sup>+</sup>/CD4<sup>+</sup>FOXP3<sup>+</sup> ratio (above the median, cut-off 13) in the stroma after NACT was associated to longer PFS.

In our study, as in others previously published, the majority of tumor-infiltrating T-cell rates after NACT were found in the stromal or peritumoral compartment, but not in the intratumoral site. This fact continues to be one of the greatest challenges in clinical practice: promote the infiltration of effective effector immune cells within the tumor enhancing cytotoxic immunity. Different approaches have been investigated to convert this tumor from “cold” to “hot” (28). In this tentative of switching tumor's immunogenicity, the addition of anti-PDL-1 to chemotherapy and bevacizumab has unfortunately failed in the first line (IMAGYN-050; ref. 9) and in the platinum-sensitive relapse (NCT02891824-ENGOT Ov29/ATALANTE; ref. 29). The limited access of CD8<sup>+</sup> T cells to the intraepithelial compartment of the tumor could be one of the reasons that may explain the lack of efficacy (30). The combination of (ADP-ribose) polymerase inhibitors (PARPi) with immune check-point inhibitors (ICI) has been postulated as a potential strategy to enhance ICI activity in EOC. The rationale for combining PARPi and anti-PD1/PD-L1 is based on preclinical observations that have shown the upregulation of PD-L1 following exposure to PARPi as well as evidence of increasing the activity of the stimulator of interferon genes (STING) and interferon pathways after niraparib administration (PARPi), which led towards an enhancing of intratumoral immune cell infiltration and upregulating granzyme B-positive T cells (31). Encouraging results of the PARPi and anti-PDL1/PD1 combination has been presented [TOPACIO/KEYNOTE-162 (32) and MEDIOLA (33)], and phase III trials trying to validate this concept in the first-line (KEYLYNK-001/ENGOT-Ov43, FIRST/ENGOT Ov44, ATHENA/GOG 3020/ENGOT Ov45, DUO-O/ENGOT Ov46) and in the platinum-sensitive relapse (ENGOT-Ov41/GEICO-69/ANITA) are awaited eagerly (34).

Our study presents a series of strengths and limitations, which would partly explain the results here obtained. First, it is worth mentioning that to our knowledge this is the first study that evaluates the changes in TME after NACT with bevacizumab and compares it with the NACT without bevacizumab. In ovarian cancer, most of the published studies in this area analyzed the changes after NACT administration but without analyzing the potential benefit of adding bevacizumab. In cervical cancer, a recent study with the same rationale detected an increase of CD8<sup>+</sup> populations after NACT combined with bevacizumab, results that are in line with the ones obtained in our study (35). In addition, we carried out an extensive characterization of tumor tissue samples by selecting at least 20 regions of the same sample and analyzing them jointly per patient. Cell-type quantification has been carried out at the same time in the same tissue slide, being able to spatially observe the localization and potential colocalization of immune populations both at the tumor and stromal level.

Regarding the limitations of the study, our main limitation is the small sample size. Initially, it was expected to collect 71 matched samples, but in the end, only 23 patient-matched samples could be collected before and after NACT. Despite this fact, the results here obtained are representative of the immunologic landscape before and after NACT, because the characteristic of the patients included in this study are similar to the original cohort ( $n = 63$ ) published in 2019 (8). These findings highlight the challenge of getting tumor tissue for translational research in clinical trials when there is not a pre-planned translational protocol. In the analysis of the immune populations, some of the values obtained were close to significance, but due, in part, to the small sample size, it has not been possible to confirm the trend obtained in such analyses. In addition, we can hypothesize that patients with better responses to chemotherapy have less residual tumor tissue for adequate analysis, which may limit the interpretation of the survival analysis.

In summary, in the GEICO1205 study, the addition of bevacizumab to NACT did not have an impact on complete cytoreduction at ICS or PFS in patients diagnosed with advanced ovarian cancer. At biological level, this combination influences CD4<sup>+</sup>, CD8<sup>+</sup> lymphocyte populations and CD8<sup>+</sup>/CD4<sup>+</sup>FOXP3 ratio at the stromal compartment, but not intratumorally, which leads us to hypothesize about the existence of mechanisms of resistance to ICI that could prevent the trafficking of T effector cells into the epithelial component of the tumor. If the combination of PARPi and ICI could prevent this potential mechanism of resistance will be elucidated by randomized phase III trials in the first-line and the recurrent setting.

### Authors' Disclosures

M. Gil-Martin reports other support from GSK and MSD outside the submitted work. M. Romeo reports other support from GSK, AZ, and MSD outside the submitted work. M.P. Barretina-Ginesta reports personal fees from Clovis, GSK, AstraZeneca, MSD, Pharmamar, and Eisai outside the submitted work. A. Manzano reports grants from AstraZeneca, personal fees and other support from GSK, personal fees from Sanofi and ROVI, and other support from MSD outside the submitted work. L. Gaba reports personal fees and nonfinancial support from GSK, MSD, AstraZeneca, and Clovis Oncology and personal fees from PharmaMar outside the submitted work. A. González-Martín reports grants and nonfinancial support from GEICO and grants

from Roche Spain during the conduct of the study as well as personal fees from Alkermes, Amgen, AstraZeneca, Clovis Oncology, Genmab, GSK, ImmunoGen, MSD, MacroGenics, Novartis, Oncoinvent, Pfizer/Merck, PharmaMar, Roche, Sotio, Sutro, Tubulis, HederDx, and Illumina outside the submitted work. No disclosures were reported by the other authors.

### Authors' Contributions

**B. Tavira:** Conceptualization, data curation, investigation, visualization, methodology, writing—original draft, writing—review and editing. **T. Iscar:** Investigation, visualization, methodology, writing—review and editing. **L. Manso:** Resources, writing—review and editing. **A. Santaballa:** Resources, writing—review and editing. **M. Gil-Martín:** Resources, writing—review and editing. **Y. García García:** Resources, writing—review and editing. **M. Romeo:** Resources, writing—review and editing. **M. Iglesias:** Resources, writing—review and editing. **A. de Juan Ferré:** Resources, writing—review and editing. **M.P. Barretina-Ginesta:** Resources, writing—review and editing. **A. Manzano:** Resources, writing—review and editing. **L. Gaba:** Resources, writing—review and editing. **M.J. Rubio:** Resources, writing—review and editing. **C.E. de Andrea:** Formal analysis, investigation, visualization, methodology, writing—review and editing. **A. González-Martín:** Conceptualization, resources, funding acquisition, writing—original draft, writing—review and editing.

### Acknowledgments

This work was supported by Foundation for Applied Medical Research (FIMA), funded by GEICO (Grupo Español en Investigación en Cáncer de Ovario) and an unrestricted grant from Roche Spain. We thank Dr. Alfonso Calvo from Universidad de Navarra and Miriam Redrado for their technical support in the early phases of this study. We also thank Cristina Sainz for the excellent technical support and sample processing. Also, to the Image Department, to Aihnoa and Mikel for the help in analyzing the images with Qu-path.

The publication costs of this article were defrayed in part by the payment of publication fees. Therefore, and solely to indicate this fact, this article is hereby marked “advertisement” in accordance with 18 USC section 1734.

### Note

Supplementary data for this article are available at Clinical Cancer Research Online (<http://clincancerres.aacrjournals.org/>).

Received March 14, 2023; revised June 8, 2023; accepted July 27, 2023; published first August 1, 2023.

### References

- Wood GE, Ledermann JA. Adjuvant and post-surgical treatment in high-grade epithelial ovarian cancer. *Best Pract Res Clin Obstet Gynaecol* 2022;78:64–73.
- Vergote I, Gonzalez-Martín A, Lorusso D, Gourley C, Mirza MR, Kurtz J-E, et al. Clinical research in ovarian cancer: consensus recommendations from the gynecologic cancer InterGroup. *Lancet Oncol* 2022;23:e374–84.
- Vergote I, Tropé CG, Amant F, Kristensen GB, Ehlen T, Johnson N, et al. Neoadjuvant chemotherapy or primary surgery in stage IIIC or IV ovarian cancer. *N Engl J Med* 2010;363:943–53.
- du Bois A, Reuss A, Pujade-Lauraine E, Harter P, Ray-Coquard I, Pfisterer J. Role of surgical outcome as prognostic factor in advanced epithelial ovarian cancer: a combined exploratory analysis of 3 prospectively randomized phase 3 multicenter trials: by the arbeitsgemeinschaft gynaekologische onkologie studiengruppe ovarialkarzinom (AGO-OVAR) and the groupe d'investigateurs nationaux pour les études des cancers de l'ovaire (GINECO). *Cancer* 2009;115:1234–44.
- Burger RA, Brady MF, Bookman MA, Fleming GF, Monk BJ, Huang H, et al. Incorporation of bevacizumab in the primary treatment of ovarian cancer. *N Engl J Med* 2011;365:2473–83.
- Perren TJ, Swart AM, Pfisterer J, Ledermann JA, Pujade-Lauraine E, Kristensen G, et al. A phase 3 trial of bevacizumab in ovarian cancer. *N Engl J Med* 2011;365:2484–96.
- Rouzier R, Gouy S, Selle F, Lambaudie E, Floquet A, Fourchette V, et al. Efficacy and safety of bevacizumab-containing neoadjuvant therapy followed by interval debulking surgery in advanced ovarian cancer: results from the ANTHALYA trial. *Eur J Cancer* 2017;70:133–42.
- García García Y, de Juan Ferré A, Mendiola C, Barretina-Ginesta M-P, Gaba García L, Santaballa Bertrán A, et al. Efficacy and safety results from GEICO 1205, a randomized phase II trial of neoadjuvant chemotherapy with or without bevacizumab for advanced epithelial ovarian cancer. *Int J Gynecol Cancer* 2019;29:1050–6.
- Moore KN, Bookman M, Sehouli J, Miller A, Anderson C, Scambia G, et al. Atezolizumab, bevacizumab, and chemotherapy for newly diagnosed stage III or IV ovarian cancer: placebo-controlled randomized phase III trial (IMagyn050/GOG 3015/ENGOT-OV39). *J Clin Oncol* 2021;39:1842–55.
- Jiménez-Sánchez A, Cybulska P, Mager KL, Koplev S, Cast O, Couturier D-L, et al. Unraveling tumor-immune heterogeneity in advanced ovarian cancer uncovers immunogenic effect of chemotherapy. *Nat Genet* 2020;52:582–93.
- Mesnage SJL, Auguste A, Genestie C, Dunant A, Pain E, Drusch F, et al. Neoadjuvant chemotherapy (NACT) increases immune infiltration and programmed death-ligand 1 (PD-L1) expression in epithelial ovarian cancer (EOC). *Ann Oncol* 2017;28:651–7.
- Zhang L, Conejo-García JR, Katsaros D, Gimotty PA, Massobrio M, Regnani G, et al. Intratumoral T cells, recurrence, and survival in epithelial ovarian cancer. *N Engl J Med* 2003;348:203–13.

13. Hamanishi J, Mandai M, Iwasaki M, Okazaki T, Tanaka Y, Yamaguchi K, et al. Programmed cell death 1 ligand 1 and tumor-infiltrating CD8+ T lymphocytes are prognostic factors of human ovarian cancer. *Proc Natl Acad Sci USA* 2007; 104:3360–5.
14. Curiel TJ, Coukos G, Zou L, Alvarez X, Cheng P, Mottram P, et al. Specific recruitment of regulatory T cells in ovarian carcinoma fosters immune privilege and predicts reduced survival. *Nat Med* 2004;10:942–9.
15. Nowak M, Klink M. The role of tumor-associated macrophages in the progression and chemoresistance of ovarian cancer. *Cells* 2020;9:1299.
16. Leary A, Genestie C, Blanc-Durand F, Gouy S, Dunant A, Maulard A, et al. Neoadjuvant chemotherapy alters the balance of effector to suppressor immune cells in advanced ovarian cancer. *Cancer Immunol Immunother* 2021;70:519–31.
17. Bankhead P, Loughrey MB, Fernández JA, Dombrowski Y, McArt DG, Dunne PD, et al. QuPath: Open source software for digital pathology image analysis. *Sci Rep* 2017;7:16878.
18. Anderson NM, Simon MC. The tumor microenvironment. *Curr Biol* 2020;30:R921–5.
19. Montfort A, Pearce O, Maniati E, Vincent BG, Bixby L, Böhm S, et al. A strong B-cell response is part of the immune landscape in human high-grade serous ovarian metastases. *Clin Cancer Res* 2017;23:250–62.
20. Böhm S, Montfort A, Pearce OMT, Topping J, Chakravarty P, Everitt GLA, et al. Neoadjuvant chemotherapy modulates the immune microenvironment in metastases of tubo-ovarian high-grade serous carcinoma. *Clin Cancer Res* 2016;22:3025–36.
21. Lo CS, Sanii S, Kroeger DR, Milne K, Talhouk A, Chiu DS, et al. Neoadjuvant chemotherapy of ovarian cancer results in three patterns of tumor-infiltrating lymphocyte response with distinct implications for immunotherapy. *Clin Cancer Res* 2017;23:925–34.
22. Blanc-Durand F, Genestie C, Galende EY, Gouy S, Morice P, Pautier P, et al. Distribution of novel immune-checkpoint targets in ovarian cancer tumor microenvironment: a dynamic landscape. *Gynecol Oncol* 2021;160:279–84.
23. García-Martínez E, Redondo A, Piulats JM, Rodríguez A, Casado A. Are antiangiogenics a good “partner” for immunotherapy in ovarian cancer? *Angiogenesis* 2020;23:543–57.
24. Napoletano C, Ruscito I, Bellati F, Zizzari IG, Rahimi H, Gasparri ML, et al. Bevacizumab-based chemotherapy triggers immunological effects in responding multi-treated recurrent ovarian cancer patients by favoring the recruitment of effector T cell subsets. *J Clin Med* 2019;8:380.
25. Lieber S, Reinartz S, Raifer H, Finkernagel F, Dreyer T, Bronger H, et al. Prognosis of ovarian cancer is associated with effector memory CD8+ T cell accumulation in ascites, CXCL9 levels and activation-triggered signal transduction in T cells. *Oncoimmunology* 2018;7:e1424672.
26. Adams SF, Levine DA, Cadungog MG, Hammond R, Facciabene A, Olvera N, et al. Intraepithelial T cells and tumor proliferation: impact on the benefit from surgical cytoreduction in advanced serous ovarian cancer. *Cancer* 2009;115:2891–902.
27. Pölcher M, Braun M, Friedrichs N, Rudlowski C, Bercht E, Fimmers R, et al. Foxp3(+) cell infiltration and granzyme B(+)/Foxp3(+) cell ratio are associated with outcome in neoadjuvant chemotherapy-treated ovarian carcinoma. *Cancer Immunol Immunother* 2010;59:909–19.
28. Blankenstein T, Coulie PG, Gilboa E, Jaffee EM. The determinants of tumour immunogenicity. *Nat Rev Cancer* 2012;12:307–13.
29. Kurtz JE, Pujade-Lauraine E, Oaknin A, Belin L, Tsubulak I, Cibula D, et al. LBA30 - phase III ATALANTE/ov29 trial: atezolizumab (Atz) versus placebo with platinum-based chemotherapy (Cx) plus bevacizumab (bev) in patients (pts) with platinum-sensitive relapse (PSR) of epithelial ovarian cancer (OC). *Ann Oncol* 2022;S808–69.
30. Gajewski TF, Meng Y, Blank C, Brown I, Kacha A, Kline J, et al. Immune resistance orchestrated by the tumor microenvironment. *Immunol Rev* 2006; 213:131–45.
31. Jiao S, Xia W, Yamaguchi H, Wei Y, Chen M-K, Hsu J-M, et al. PARP inhibitor upregulates PD-L1 expression and enhances cancer-associated immunosuppression. *Clin Cancer Res* 2017;23:3711–20.
32. Konstantinopoulos PA, Waggoner S, Vidal GA, Mita M, Moroney JW, Holloway R, et al. Single-arm phases 1 and 2 trial of niraparib in combination with pembrolizumab in patients with recurrent platinum-resistant ovarian carcinoma. *JAMA Oncol* 2019;5:1141–9.
33. Domchek SM, Postel-Vinay S, Im S-A, Park YH, Delord J-P, Italiano A, et al. Olaparib and durvalumab in patients with germline BRCA-mutated metastatic breast cancer (MEDIOLA): an open-label, multicentre, phase 1/2, basket study. *Lancet Oncol* 2020;21:1155–64.
34. Gonzalez Martin A, Sanchez Lorenzo L, Colombo N, dePont Christensen R, Heitz F, Meirovitz M, et al. A phase III, randomized, double blinded trial of platinum based chemotherapy with or without atezolizumab followed by niraparib maintenance with or without atezolizumab in patients with recurrent ovarian, tubal, or peritoneal cancer and platinum treatment free interval of more than 6 months: ENGOT-Ov41/GEICO 69-O/ANITA trial. *Int J Gynecol Cancer* 2021;31:617–22.
35. Boucher Y, Kumar AS, Posada JM, Gjini E, Pfaff K, Lipschitz M, et al. Bevacizumab improves tumor infiltration of mature dendritic cells and effector T-cells in triple-negative breast cancer patients. *NPJ Precis Oncol* 2021;5:62.